Quantized Spin Waves in the Metallic State of Magnetoresistive Manganites

S. Petit,[1] M. Hennion,[1] F. Moussa,[1] D. Lamago,[1,2] A. Ivanov,[3] Y. M. Mukovskii,[4] and D. Shulyatev[4]

[1]*Institut Rayonnement Matière de Saclay, Laboratoire Léon Brillouin, CEA-CNRS UMR 12, CE-SACLAY, F-91191 Gif sur Yvette Cedex, France*

[2]*Forschungzentrum Karlsruhe, INFP, P.O. Box 3640, D-76021 Karlsruhe, Germany*

[3]*Institut Laue Langevin, 156X, 38042 Grenoble cedex 9, France*

[4]*Moscow State Steel and Alloys Institute, Moscow 119049, Russia*

(Received 5 December 2008; published 18 May 2009)

Spin wave measurements have been carried out in ferromagnetic (F) $La_{1-x}(Sr, Ca)_xMnO_3$ with $x(Sr) = 0.15, 0.175, 0.2, 0.3$, and $x(Ca) = 0.3$. In all q directions, close to the zone boundary, the spin wave spectra consist of several energy levels, with the same values in the metallic and the $x \approx 1/8$ doping ranges. For $x(Sr) = 0.15$, the data are quantitatively interpreted in terms of quantized spin waves within 2D ordered F domains or clusters of $4a$ size. The same picture holds in the metallic state with, however, disordered clusters embedded in a 3D F matrix.

DOI: 10.1103/PhysRevLett.102.207201 PACS numbers: 75.30.Ds, 05.70.−a, 73.23.Ad

The discovery of colossal magnetoresistance (CMR) in cubic manganites, along with the nature of their metallic ferromagnetic (F) phase, have aroused a lot of experimental and theoretical research interest for the last decade [1–3]. A large number of studies have been devoted to the description of the evolution of spin dynamics in these materials, starting from the orbitally ordered (OO) insulating $LaMnO_3$ to the orbitally disordered (OD) metallic $La_{1-x}B_xMnO_3$. For these last compositions, several anomalies have been identified in the spin wave spectra, which are suggested to be generic features of the unusual metallic state of CMR manganites [4–6]. As these unconventional spin waves remain unexplained, new experimental efforts are needed to extend our understanding of these compounds and of their puzzling properties.

In this context, we have performed measurements of spin wave excitations in five $La_{1-x}B_xMnO_3$ samples, B = Sr or Ca, for dopings covering a large part of the phase diagram (see Fig. 1), from the quasimetallic (zone 2) and insulating (zone 3 or O′O″ phase) parts with $x(Sr) = 0.15$ to the metallic part with $x(Sr) = 0.175$, 0.2, 0.3 and $x(Ca) = 0.3$ (zone 4).

For all dopings, the magnetic excitation spectrum consists of a quadratic dispersed curve at the zone center, characteristic of a three-dimensional (3D) ferromagnetic state, and wave-vector–independent levels at the zone boundary. These levels are roughly identical whatever the doping content (zones 2, 3, 4), the temperature T, or the average cation size r_a [7]. Their intensity depends, however, on x, T, or r_a and is found to jump from the lower ones (≈15, 22 meV along [100]), to the upper ones (≈32, 41, 51 meV) as x increases from $\approx 1/8$ to the metallic state. As first proposed in [8], the *lower* levels can be interpreted in terms of quantized spin waves within 2D F domains or clusters of $4a$ size, considered as residual effects of the orbital ordering. For $x \approx 1/8$, at low T, these clusters order to form a ferromagnetic striped phase. We propose that the *upper* ones arise from the hybridization of those quantized spin waves with a 3D F matrix, surrounding the disordered clusters. By defining J_{OD} and J_{OO} as the nearest neighbors (NN) couplings in the matrix and in the clusters, respectively, we find that J_{OD} increases with doping while J_{OO} remains approximately constant, so that $J_{OD} \leq J_{OO}$ in zone 2 and $J_{OD} \geq J_{OO}$ in zone 4. As J_{OD} is a measure of the stiffness constant $\mathcal{D}$ and in turn of the metallic coupling, this rapid variation with x or T is quite natural. Moreover, we claim that this picture explains the apparent softening of the spin wave spectrum [4–6].

Inelastic neutron scattering measurements have been carried out at the Laboratoire Léon Brillouin (1T, 2T, 4F spectrometers) and at the Institut Laue Langevin (*IN*8 spectrometer). PG_{002} was used as analyzer, together with Cu_{111}, Cu_{002}, Cu_{220}, or PG_{002} as monochromators, yielding an energy resolution (FWHM) varying from 1.5 to 4 meV at intermediate energy transfer $E = 16$ meV. Data were

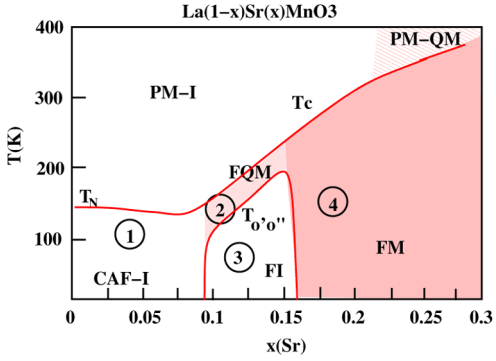

FIG. 1 (color online). Schematic phase diagram of $La_{1-x}Sr_xMnO_3$. Zone 1: insulating canted antiferromagnetic state. Zone 2: ferromagnetic quasimetallic state. Zone 3: insulating ferromagnetic state. Zone 4: metallic ferromagnetic state.

fitted by Lorentzian line shapes convoluted with instrumental resolution, allowing the determination of the intrinsic linewidth Γ.

All samples have an orthorhombic structure except $La_{0.7}Sr_{0.3}MnO_3$ which is rhombohedral. For simplicity, the wave vector Q is defined in pseudocubic indexation with a, b, c directions and a ($\approx$3.9 Å) as lattice spacing. In the quasimetallic and insulating states of $La_{0.85}Sr_{0.15}MnO_3$ where the magnetic coupling is anisotropic, we consider that, by continuity with $LaMnO_3$, a and b are equivalent whereas c is distinct. There, due to twinning, the [100], [010], [001] directions are superimposed whereas the [111] direction corresponds to a single domain.

We first describe the spin dynamics in zones 2 and 3 of the phase diagram. Here, the spin wave spectrum of $x(\mathrm{Sr}) = 0.15$ along $[1 + q, 0, 0]$ is found to be very close to that observed for $x(\mathrm{Sr}) = 0.125$ [8]. Below $T_C = 230$ K, a quadratic $E = \mathcal{D}q^2$ dispersion is observed for $q \leq 0.25$, as well as several q-independent levels for $q > 0.25$. Below $T_{O'O''} = 180$ K, $\mathcal{D}$ increases, and a gap opens at $q = 0.125$. Concomitantly, the levels become q modulated. Figures 2(a) and 2(b) show examples of raw data taken at $T = 14$ K, for $q = 0.25$ and $q = 0.5$. The arrows point three resolved levels, lying at $E = 7.5$, 15, 23 meV for $q = 0.5$. The mode at $E \approx 31$ meV in the shoulder of the main peak will be discussed below. Figures 2(c) and 2(d) show the spin wave spectra along [100] and [111], respectively. We observe that the energies of the zone boundary modes with strongest intensity differ by a factor of $\approx$2, which is expected for a 2D coupling. Actually, the data provide evidence for two new features, not observed before [9]. (i) Along $[1 + q, 0, 0]$ with $q = 0.125$, three modes are detected [cf. Figs. 2(c) and 2(c′)]. Because of its x and T variation, the low-energy curve observed only for $q < 0.15$, is assigned to the c direction. As a result, both a and b directions are concerned with the gap opening. (ii) Along [111], six levels are resolved beyond the small-q dispersion [Fig. 2(d)]. In a recent paper [8], we proposed a qualitative interpretation of this spin wave spectrum in terms of quantized spin waves in 2D $4a \times 4a$ ferromagnetic clusters. We have improved this description assuming the existence of a long-range ordering of such small clusters in (a),(b) planes, and resulting in the orthogonal-stripes picture sketched in Fig. 3(a). In the absence of experimental indication, the ordered 2D clusters are supposed to be disordered along c. To calculate the

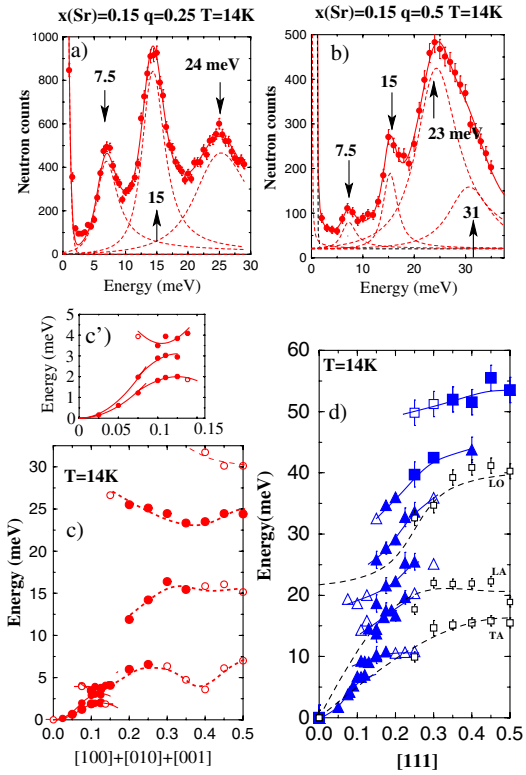

FIG. 2 (color online). Spin waves determination in $La_{0.85}Sr_{0.15}MnO_3$ at 14 K. (a) and (b) are examples of energy spectra at $Q = (1.25, 0, 0)$ and (1.5,0,0) respectively, (c) and (d) are spin wave spectra along $[100] + [010] + [001]$ and [111] respectively, with, in (c'), a zoom of the low energy part of (c). The full (empty) color of the symbols indicates large (weak) intensity. In (d), triangles (squares) indicate measurements in second (third) Brillouin zones. The black squares are phonons measured with magnons in the third Brillouin zone.

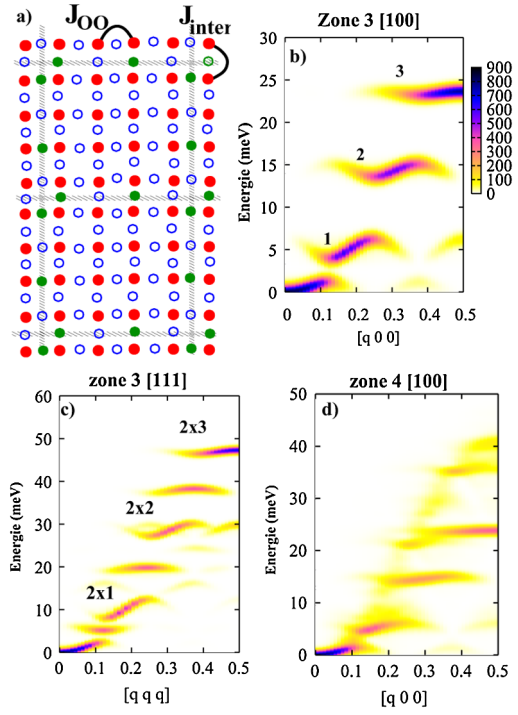

FIG. 3 (color online). (a) schematic drawing of two units of the 2D stripe model with red or solid gray (blue or open gray and green or solid dark gray) circles for Mn (O and O + hole). (b), (c),(d) calculated spin wave spectra (see the text). (b) zone 3, along [100], (c) zone 3, along [111], (d) zone 4, along [100] using 44×44 spins in (a),(b) plane and 5 planes with cyclic boundary conditions.

spin dynamics, we consider a Heisenberg model with two NN interactions, J_{OO} and J_{inter}, that couple, respectively, Mn spins within the same cluster and across the cluster boundaries [cf. Fig. 3(a)]. This kind of superstructure, also proposed in the context of high-T_C [10], implies that the holes lie, in average, on the oxygen (O) atoms of the boundaries. Note that $x = 1/8$ precisely corresponds to half-filling [see Fig. 3(a)], which may explain the stability of the O′O″ phase. For $J_{inter} = 0$, the spin dynamics is that of quantized spin waves within $4a \times 4a$ clusters. 16 levels are expected at energies given by $E_{x,y} = 4J_{OO}S(1 - \frac{\cos\frac{\pi x}{n}+\cos\frac{\pi y}{n}}{2})$, with $n = 4$ and $x, y = 0, \ldots, 3$. If $J_{inter} \lesssim J_{OO}$, the quantized spin waves in different clusters couple, and the levels become weakly dispersive. Choosing $J_{inter} = J_{OO}/5$ allows a *quantitative* description of the data, at least for $q \geq 0.15$ [Figs. 3(b) and 3(c)]. Because of the cluster square symmetry, three levels along [100] and six along [111] can be observed, in good agreement with experiment. Discrepancies appear for $q < 0.15$ along [100] (too large gap at $q = 0.125$) and along [111] (calculated energy values smaller than observed). This may indicate that another F coupling coexists, giving rise to the nearly isotropic dispersion seen for $q \leq 0.15$ [cf. Fig. 2(c)]. Equivalently, it may suggest that the 2D ordering of the clusters coexists with a metallic component [11]. Before going further, we point out that our confidence in this model, which differs from that based on structural properties [12,13], arises from the agreement found for both the [100] and [111] directions. Actually, a similar spin dynamics is observed for Ca and Ba substitution within the zone 3, although their structural properties are different: an incommensurate superstructure peak is found for $x(\mathrm{Sr}) = 0.15$, whereas for $x(\mathrm{Ca}) = 0.17$ and $x(\mathrm{Ba}) = 0.15$ short-range structural defects are observed ([14] and to be published).

On entering the metallic side (zone 4), we argue that the same physics is at play. We observe indeed strong similarities with the $x \approx 1/8$ range. Again, as shown on Fig. 4, the spin wave spectra consist of two components: a quadratic regime near the zone center and several levels close to the zone boundary. Figure 4 shows representative raw data taken at $Q = (1.5, 0, 0)$ for 298, 250, 150, and 14 K in the $x(\mathrm{Sr}) = 0.3$ compound ($T_C = 370$ K). The two levels at 15 and 22 meV typical of the $x \approx 1/8$ range, are properly resolved (full arrows in Fig. 4), together with new ones lying at $E \approx 32$ meV, ≈ 41 meV, and ≈ 51 meV (empty arrows). As the temperature decreases, the intensity progressively shifts from the two low-energy levels towards

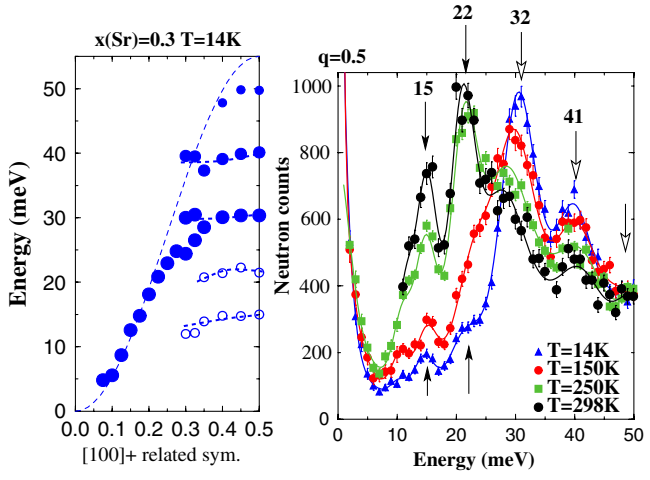

FIG. 4 (color online). Left panel: spin wave dispersion for $x(\mathrm{Sr}) = 0.3$. The full (empty) circles correspond to large (weak) intensity. The dashed line points out the softening effect. Right panel: raw data for $Q = (0, 0, 1.5)$ at five T values. Solid lines are fits from which Γ values ($\Gamma \approx 0.5$) are determined. Full arrows point modes typical of the $x \approx 1/8$ range and empty ones, the new ones observed in the metallic state.

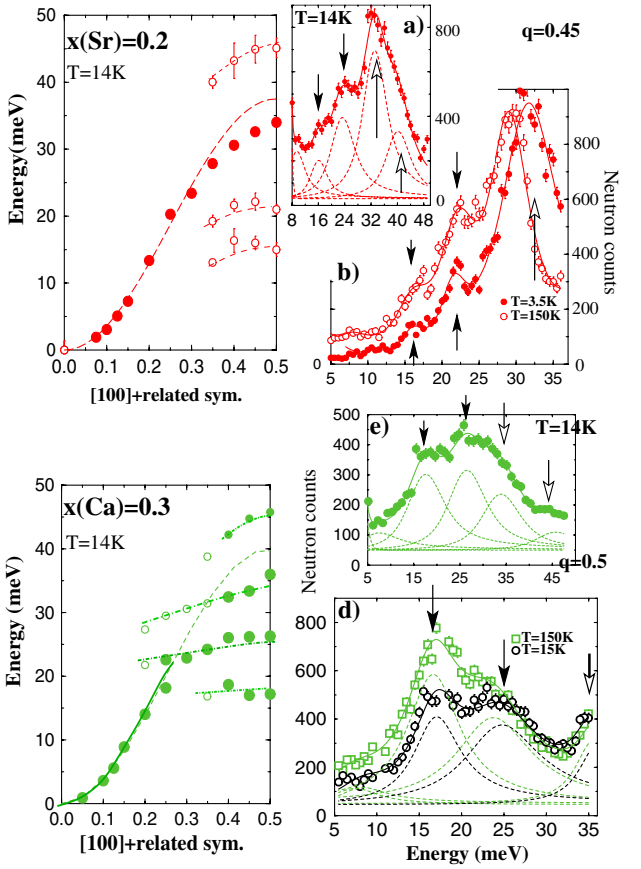

FIG. 5 (color online). Left panel: spin wave dispersions for $x(\mathrm{Sr}) = 0.2$ (top) and $x(\mathrm{Ca}) = 0.3$ (bottom) at $T = 14$ K. The full (empty) circles correspond to large (weak) intensity. The dashed lines point out the softening effect. Right panel: corresponding data at several T for $q = 0.45$ [$x(\mathrm{Sr}) = 0.2$] and $q = 0.5$ [$x(\mathrm{Ca}) = 0.3$] using $E_f = 14.7$ meV (b),(d) and $E_f = 35$ meV (a),(b). Solid lines are fits from which $\Gamma \approx 0.7$ and ≈ 6 meV are determined for the modes in $x(\mathrm{Sr}) = 0.2$ and $x(\mathrm{Ca}) = 0.3$, respectively. Full and empty arrows have the same meaning as in Fig. 4.

the higher energy ones. This evolution can be correlated with the concomitant increase of the stiffness constant $\mathcal{D}$. Along [111], new levels are observed above 50 meV up to $\approx$90–100 meV, which reveal a 3D coupling. This will be reported elsewhere. Similar results are observed for other dopings within the metallic regime (zone 4), namely, for $x(\mathrm{Sr}) = 0.175$ ($T_C = 270$ K), $x(\mathrm{Sr}) = 0.2$ ($T_C = 325$ K), and $x(\mathrm{Ca}) = 0.3$ ($T_C = 255$ K). The upper and lower panel of Fig. 5 show the corresponding spin wave spectra obtained for $x(\mathrm{Sr}) = 0.2$ and $x(\mathrm{Ca}) = 0.3$, together with raw data measured at the zone boundary. Because of experimental limitations, the maximum available energy transfer $E_{\max}$ increases with the final energy of the neutrons E_f, while the energy resolution rapidly drops. The low energy levels around 15–17 meV and 22–25 meV are thus well resolved with $E_f = 14.7$ meV ($E_{\max} <$ 35 meV), as shown on Fig. 5(b) and 5(d), right panel. Those at higher energy are detected with $E_f = 35$ meV ($E_{\max} < 51$ meV), see Figs. 5(a) and 5(c), with, however, a coarse resolution. For $x(\mathrm{Ca}) = 0.3$ where $\Gamma \approx 6$ meV is large, the agreement found between the two fits ensures the stability of the analysis. For all dopings, as T increases, the intensity of the low energy levels increases, whereas those at higher energy decreases. This temperature dependence is thus a general trend. We also note that for $x(\mathrm{Ca}) = 0.3$, the levels have comparable intensity even at low temperature. This contrasts with the $x(\mathrm{Sr}) = 0.3$ case, but should be correlated with the different $\mathcal{D}$ value (150 and 200 meV Å^2, respectively) and T_C value observed in these two compounds.

These observations in the metallic state can be understood in an extended version of the above mentioned model. We now assume disordered 2D F clusters of $4a \times 4a$ size, embedded in a 3D F matrix and take into account the ferromagnetic NN coupling J_{OD}, acting between spins within this 3D medium. Basically, J_{OD} has the same physical meaning as $\mathcal{D}$ ($J_{\mathrm{OD}} = \mathcal{D}/2Sa^2$) induced by hopping electrons. A qualitative agreement between experiment and numerical simulations is obtained if $J_{\mathrm{OD}} \geq J_{\mathrm{OO}}$. Figure 3(d) shows an example of calculated spin wave spectrum along [100] performed with a density of clusters of 50%, $J_{\mathrm{OD}} = 1.75 J_{\mathrm{OO}}$ ($J_{\mathrm{OO}} = 1.7$ meV) and $J_{\mathrm{inter}} = J_{\mathrm{OO}}/5$. The calculation shows levels which are clearly reminiscent of quantized spin waves within the clusters, but the hybridization with the 3D medium blurs the large gaps at low q and adds new levels at higher energy. Actually, the weak $E \approx 31$ meV level detected in the $x \approx 1/8$ range below $T_{O'O''}$ [see Figs. 2(b) and 2(c)] [9] could be also due to this effect, namely, a metallic component coexisting with the insulating "charge-ordered" state, in agreement with NMR spectroscopy [11]. Finally, we note that as a function of doping, J_{OO} is found to remain approximately constant, while in contrast, J_{OD} (as $\mathcal{D}$) is found to increase, as expected in a metallic system.

This interpretation provides also a simple explanation for the so-called "softening" effect. As shown by the dashed lines on the left panel of Figs. 4 and 5, the cosine law expected from conventional double-exchange model [15], defined from the $q \approx 0$ dispersion, yields a zone boundary energy value clearly above the experimental one. Previous studies have proposed that this anomaly may be due to fourth neighbor coupling term [4–6], assuming the existence of a single branch. Our observations, however, unveil cluster excitations characterized by J_{OO}. As $J_{\mathrm{OD}} \geq J_{\mathrm{OD}}$, this causes an apparent "softening" of the zone boundary energy. Note that our interpretation reproduces the experiments in zone 2 with $J_{\mathrm{OD}} \leq J_{\mathrm{OO}}$ [8].

In conclusion, these data show that the metallic state of manganites can be described in terms of quantized spin waves in 2D clusters embedded in a 3D matrix. The remarkable similarities of the spin dynamics observed in several compounds indicate that these inhomogeneities have the same origin whatever T, x, or the average cation size. These new observations correlate well with other properties of these compounds such as the residual resistivity [16] and the distinct magnetic time scales far from T_C [17]. Moreover, we speculate that this description provides a new insight around T_C, where magnetic anomalies have been observed [18,19] and, hence, in the giant magnetoresistance properties of these compounds.

[1] *Nanoscale Phase Separation and Colossal Magnetoresistance*, edited by E. Dagotto (Springer-Verlag, Berlin, 2002).
[2] Y. Motome and N. Furukawa, Phys. Rev. B **71**, 014446 (2005).
[3] Sanjeev Kumar *et al.*, Phys. Rev. Lett. **97**, 176403 (2006).
[4] Y. Endoh *et al.*, Phys. Rev. Lett. **94**, 017206 (2005).
[5] F. Ye *et al.*, Phys. Rev. Lett. **96**, 047204 (2006); Phys. Rev. B **75**, 144408 (2007).
[6] F. Moussa *et al.*, Phys. Rev. B **76**, 064403 (2007).
[7] H. Y. Hwang *et al.*, Phys. Rev. Lett. **75**, 914 (1995).
[8] M. Hennion *et al.*, Phys. Rev. B **73**, 104453 (2006).
[9] F. Moussa *et al.*, Phys. Rev. B **67**, 214430 (2003).
[10] Boris Fine, arXiv:cond-mat/0404488.
[11] G. Papavassiliou *et al.*, Phys. Rev. Lett. **96**, 097201 (2006).
[12] Y. Yamada *et al.*, Phys. Rev. Lett. **77**, 904 (1996)
[13] J. Geck, Phys. Rev. Lett. **95**, 236401 (2005).
[14] Pencheng Dai *et al.*, Phys. Rev. Lett. **85**, 2553 (2000).
[15] N. Furukawa J. Phys. Soc. Jpn. **65**, 1174 (1996).
[16] J. M. D. Coey *et al.*, Phys. Rev. Lett. **75**, 3910 (1995).
[17] R. H. Heffner *et al.*, Phys. Rev. Lett. **77**, 1869 (1996).
[18] J. W. Lynn *et al.*, Phys. Rev. Lett. **76**, 4046 (1996).
[19] L. Vasiliu-Doloc *et al.*, J. Appl. Phys. **83**, 7342 (1998).